Cortical network fingerprint and prediction of deep brain stimulation-induced speech impairment in essential tremor

Jan Niklas Petry-Schmelzer,[1,*] Hannah Jergas,[1,*] Tabea Thies,[2,1] Julia K. Steffen,[1] Paul Reker,[1] Haidar S. Dafsari,[1] Doris Mücke,[2] Gereon R. Fink,[1,3] Veerle Visser-Vandewalle,[4] Till A. Dembek,[1] Michael T. Barbe[1]

*These authors contributed equally to this work

[1]University of Cologne, Faculty of Medicine and University Hospital Cologne, Department of Neurology, Cologne, Germany
[2]University of Cologne, Faculty of Arts and Humanities, Department of Linguistics, IfL Phonetics, Cologne, Germany
[3]Cognitive Neuroscience, Institute of Neuroscience and Medicine (INM-3), Research Center Jülich, Jülich, Germany
[4]University of Cologne, Faculty of Medicine and University Hospital Cologne, Department of Stereotactic and Functional Neurosurgery, Cologne, Germany

Character count title: 102/100
Character count running head: 34/40
Number of references: 67
Number of tables and figures: 6 (+1 Supplementary)
Word count abstract: 384/400
Word count introduction: 440
Word count discussion: 1769
Word count text: 4769/6000
Running head: Networks in DBS-induced dysarthria

Corresponding Author:
Jan Niklas Petry-Schmelzer
Department of Neurology
University Hospital Cologne
Kerpenerstr. 62
50924 Cologne, Germany
Tel: +49 221 478-84791
E-Mail: jan.petry-schmelzer@uk-koeln.de

Author contributions

JNPS, HJ, TT, TAD, and MTB contributed to the conception and design of the study; JNPS, HJ, TT, JKS, PR, HSD, DM, GRF, VVV, TAD and MTB contributed to the acquisition and analysis of the data; JNPS, HJ and TAD, contributed to drafting the text and preparing the figures. All authors reviewed and revised the manuscript for intellectual content.

Author disclosures

Jan Niklas Petry-Schmelzer reports travel grants from Boston Scientific.

Hannah Jergas has no financial disclosures.

Tabea Thies has no financial disclosures.

Julia Katharina Steffen reports travel grants from Boston Scientific.

Paul Reker reports a trevel grant from AbbVie.

Haidar S. Dafsari has no financial disclosures.

Doris Mücke has no financial disclosures.

Gereon R. Fink has no financial disclosures.

Veerle Visser-Vandewalle reports financial support from Boston Scientific and Medtronic for taking part in advisory board meetings, giving talks at international congresses, and for the organisation of congresses and workshops.

Till A. Dembek reports speaker's honoraria from Boston Scientific and Medtronic.

Michael T. Barbe received speaker's honoraria from Medtronic, Boston Scientific, Abbott (formerly St. Jude), GE Medical, UCB, Apothekerverband Köln e.V. and Bial as well as research funding from the Felgenhauer-Stiftung, Forschungspool Klinische Studien (University of Cologne), Horizon 2020 (Gondola), Medtronic (ODIS), and Boston Scientific and advisory honoraria for the IQWIG.

Abstract

Thalamic deep brain stimulation (DBS) is an effective treatment for patients with medically refractory essential tremor. However, stimulation-induced side-effects, especially stimulation-induced dysarthria (SID), interfere severely with quality of life and postoperative tremor control. Here, we present a functional and structural network approach to SID to gain insights into the associated brain areas and to predict stimulation-induced worsening of intelligibility. Monopolar reviews were conducted in 14 essential tremor patients with bilateral thalamic DBS by increasing the stimulation amplitude contact-wise until (i) a maximum of 10mA, (ii) the occurrence of intolerable side effects, or (iii) the onset of SID**.** Speech assessments included intelligibility ratings when reading a German standard text and a fast syllable repetition task. To detect brain areas associated with SID, a functional connectivity difference image of volumes of tissue activated (VTAs) causing SID, and VTAs not causing SID was created employing a state-of-the-art functional connectome, Lead-DBS, as well as the SPM toolbox. Additionally, discriminative fibers for stimulation-induced worsening of intelligibility were identified in a structural connectome using linear mixed effect models and validated in a leave-one-out design. A total of 111 contact assessments were included for further analysis. The functional connectivity difference image indicated stronger connectivity of VTAs causing SID (N = 51) to the precentral gyrus with a positive medio-lateral gradient, parts of the inferior and medial frontal gyrus, the supramarginal gyrus, the superior temporal gyrus, as well as the superior and the inferior cerebellar lobules, and the vermis. In the thalamic region, discriminative fibers for stimulation-induced worsening of intelligibility were located antero-laterally to fibers associated with tremor control as published by Al-Fatly et al. (2019). The overlap of the respective clinical stimulation setting's VTAs with these fibers explained 33.2% of the variance of individual change in intelligibility compared to "OFF stimulation" in a leave-one-out design. This study demonstrates that SID in essential tremor patients is related to a modulation of the functional connectome of speech production by thalamic DBS. In spite of the

proximity of functional and structural connectivity patterns for tremor control, as identified by Al-Fatly et al. (2019), and deterioration of speech, as identified in the present study, we were able to derive a fiber-based atlas structure, that could help to avoid SID in essential tremor patients. These findings might contribute to future lead placement and postoperative programming strategies.

Keywords: thalamic deep brain stimulation, speech motor system, intelligibility, dysarthria, volume of tissue activated

Abbreviations

DBS = deep brain stimulation, **DDK** = diadochokinesis, **SID** = stimulation-induced dysarthria, **PSA** = posterior subthalamic area, **STN** = subthalamic nucleus, **TRS** = tremor rating scale, **VIM** = ventral intermediate nucleus, **VTA** = volume of tissue activated

Introduction

Essential tremor is the most common adult movement disorder with an estimated prevalence of nearly 5% in populations over 65years (Louis and Ferreira, 2010). For medication refractory cases, deep brain stimulation (DBS) of the ventral intermediate nucleus of the thalamus (VIM) and the posterior subthalamic area (PSA) is an established, effective, and safe treatment (Schuurman *et al.*, 2000; Barbe *et al.*, 2018). However, side effects such as stimulation-induced dysarthria (SID), ataxia, and muscle contractions may occur (Fytagoridis *et al.*, 2013). Among these, SID is one of the most common and disabling side effects, affecting 9% (Flora *et al.*, 2010) to 75% of the patients (Pahwa *et al.*, 2006), interfering with quality of life and social functioning. Unfortunately, SID also impacts tremor control, as it often leads to suboptimal stimulation settings to avoid speech problems.

The hypothesized pathogenesis of SID is a modulation of cerebellothalamic fibers (Astrom *et al.*, 2010; Fenoy *et al.*, 2017) and connections from the motor cortex, i.e., the internal capsule (Mahlknecht *et al.*, 2017; Prent *et al.*, 2019), leading to a functional impairment of the speech motor system and hence a deterioration of speech intelligibility. While these studies examined patients with Parkinson's disease, previous studies by our group also showed an impairment of the speech motor system in essential tremor patients with thalamic DBS. Thalamic DBS led to an impairment of articulatory coordination patterns, probably due to a modulation of cerebellothalamic connections (Mücke *et al.*, 2018). Moreover, we observed articulatory imprecision and slowness affecting the production of the entire syllable cycle, most likely related to a modulation of the internal capsule (Mücke *et al.*, 2014; Becker *et al.*, 2017; Hermes *et al.*, 2019). However, the exact pathogenesis of SID remains elusive. Therefore, the first aim of the present study was to investigate the hypothesized anatomical correlates of SID.

Besides exploring the origin of SID, there is an urgent need to establish strategies to avoid SID while maintaining effective tremor control. Several approaches aimed at optimizing

postoperative tremor control including probabilistic stimulation maps (Dembek *et al.*, 2017), connectivity profiles associated with tremor control (Al-Fatly *et al.*, 2019), or the identification and direct targeting of fiber tracts associated with beneficial outcomes, e.g. the dentatorubrothalamic tract (Coenen *et al.*, 2014; Fenoy and Schiess, 2017). Regarding the avoidance of SID, previous studies focused on the influence of lead placement and stimulation settings (Barbe *et al.*, 2014; Matsumoto *et al.*, 2016; Becker *et al.*, 2017), and included dysarthria as a dichotomized symptom. In the present study, we chose speech intelligibility as the primary outcome parameter in order to predict the deterioration of speech under DBS. This measurement reflects real-life speech impairment and has been elaborated as a valid parameter for stimulation-induced impairment of the speech motor system (Mücke *et al.*, 2014; Becker *et al.*, 2017; Becker *et al.*, 2020). By combining measurements of speech intelligibility with a state-of-the-art normative connectome approach, we aimed to identify fibers predicting stimulation-induced worsening of intelligibility. These fibers might then serve as supportive atlas structures, especially for postoperative programming sessions, to avoid the occurrence of SID while maintaining effective tremor control.

Methods

Patient selection and ethics

Inclusion criteria were a confirmed diagnosis of medically intractable essential tremor according to the International Parkinson and Movement Disorder Society consensus diagnostic criteria (Deuschl *et al.*, 1998), bilateral thalamic DBS implantation (VIM or VIM/PSA) at least three months before study participation, age >18 and <80 years, and German as native language. The occurrence of postoperative SID was not an inclusion criterion, and patients were not tested for voice tremor under inactivated stimulation before study participation. The study was carried out following the Declaration of Helsinki and was approved by the local ethics committee (17-425). All patients gave written informed consent before study participation.

Clinical assessment

First, patients were assessed in "ON stimulation" state, with their regular stimulation settings as optimized per clinical routine, and in the "OFF stimulation" state after turning the stimulation off for at least 15 minutes. Second, a hemisphere-wise monopolar review was conducted with stimulation of the contralateral hemisphere turned off. When leads with eight contact heights had been implanted (Vercise™ leads, Boston Scientific), only every second contact, beginning at the tip, was included in the testing to increase spatial distribution and to diminish the examination time needed. All other leads (Cartesia™ leads, Boston Scientific, Medtronic 3387/3389 leads, Medtronic) were tested at each of the four contact heights, with circular stimulation mode for directional contacts. Contacts were tested in randomized order to maintain blinding of the examiner and the patient to the order of the tested contacts. The frequency was set to 130 Hz and a pulse width of 60 µs was chosen for every patient. Before testing, impedances were measured to ensure the integrity of the DBS system and constant current mode was set if applicable.

Monopolar reviews were performed by increasing the stimulation amplitude in steps of 0.5 mA until (i) a maximum of 10mA, (ii) the occurrence of intolerable side effects, or (iii) the onset of SID**.** The onset of SID was determined by a trained examiner (JNPS), asking the patient to enumerate the names of the months repeatedly at each amplitude step. Furthermore, contralateral muscle contractions and ataxia, defined as contralateral dysmetria during the finger-to-nose test (Groppa *et al.*, 2014), were documented.

The following clinical assessments were conducted in the (i) "ON stimulation" state, (ii) "OFF stimulation" state, and (iii) at each contact's maximum stimulation amplitude as defined during the monopolar review.

Tremor assessment. In the "ON stimulation" and "OFF stimulation" state, tremor severity was measured based on the Tremor Rating Scale (TRS). To shorten the duration of testing, tremor

severity during the monopolar review was determined by the rater as postural tremor control of the contralateral arm, rated on an open visual analogue scale (VAS) ranging from 0 cm ("no tremor") to 10 cm ("most severe tremor").

Speech assessment. In each condition, patients were asked to enumerate the months and rate their "ability to speak" on an open VAS ranging from 0 cm ("normal") to 10 cm ('worst"). The examiner was kept blinded to the patient's VAS rating throughout the testing. Then acoustic recordings in a sound-attenuated booth were conducted, including fast syllable repetition tasks (oral diadochokinesis, DDK) and natural sentence production. DDK is a standard task in which speakers were instructed to produce consonant-vowel-sequences as clearly, quickly and often as possible in one single breath. The examiner demonstrated the task before the beginning of the first recording. Syllables with velar stop consonants requiring complex tongue body movements, /kakaka/, were used, as it has been shown that they reliably reflect stimulation-induced impairments of glottal and oral speech motor control in essential tremor patients treated with DBS (Mücke *et al.*, 2014; Becker *et al.*, 2017). For natural sentence production patients were instructed to read a German standard text ("Nordwind und Sonne"/ "Northwind and Sun") at a comfortable speech rate (Becker *et al.*, 2017; Becker *et al.*, 2020).

Intelligibility ratings and DDK analysis. To investigate speech intelligibility perceived by naïve listeners (all German native speakers), we extracted the sentence with the fewest reading errors from the natural sentence production task as auditive stimuli. These were normalized to the same overall intensity level to minimize an effect of stimulus loudness on perception results. Eleven naïve listeners rated the stimuli in a randomized order across the conditions but matched for patients to ensure blinding of the listeners to the stimulation condition. Each stimulus was evaluated on an open scale reaching from 1 point ("very bad intelligibility") to 101 points ("very good intelligibility"). For further analysis intelligibility rating per stimuli was calculated as the mean of all ratings across listeners.

The DDK labeling was carried out in a blinded manner by an experienced phonetician (TT), as described previously (Becker *et al.*, 2017). In brief, syllable durations for each /ka/ sequence were identified from the start of the consonantal closure to the end of the vocalic opening with respect to the energy in the higher formant structure in the acoustic waveform. Prolonged syllable durations reflect an overall slowing down of the speech motor system and can be directly related to motor speech impairment (Ackermann *et al.*, 1995). The parameter has previously been shown to have a significant effect on intelligibility ratings and to be worsened by thalamic DBS in essential tremor patients (Becker *et al.*, 2017; Becker *et al.*, 2020).

Localization of DBS leads and volume of tissue activated estimation

DBS leads were localized with the Lead-DBS toolbox (www.lead-dbs.org) (Horn *et al.*, 2019). The detailed processing pipeline has been described elsewhere (Horn *et al.*, 2017). In brief, postoperative CT images (IQon Spectral CT, iCT 256, Brilliance 256, Philips Healthcare) were linearly co-registered to preoperative MRI (3T Ingenia, Achieva, 1.5T Ingenia, Philips Healthcare) using advanced normalization tools (ANTs, http://stnava.github.io/ANTs/, N = 13) (Avants *et al.*, 2008) or BRAINSFIT (https://github.com/BRAINSia/BRAINSTools, N = 1) (Johnson *et al.*, 2007) if ANTs did not provide sufficient results after visual inspection (Petry-Schmelzer *et al.*, 2019). Then images were nonlinearly normalized into standard space (ICBM 2009b NLIN, Asym) using ANTs and the “effective (low variance)” strategy as implemented in Lead-DBS (Ewert *et al.*, 2019). DBS leads were automatically pre-reconstructed with the PaCER-algorithm (Husch *et al.*, 2018), manually refined, and corrected for postoperative brain shift as implemented in Lead-DBS. The orientation of directional leads was determined by the DiODE algorithm (Dembek *et al.*, 2019a).

For each stimulation setting, volumes of tissue activated (VTA) were calculated in the patient’s native space and then transformed into standard space based on the individual nonlinear normalization. As in previous studies of our group (Petry-Schmelzer *et al.*, 2019), a finite element method as introduced by Horn et al. (Horn *et al.*, 2017) was employed to estimate the

spread of the electric field for homogenous tissue with a conductivity of σ = 0.1 S/m (Astrom *et al.*, 2015). The VTA was thresholded at the electrical field isolevel of 0.19 V/mm (Astrom *et al.*, 2015) to reflect clinical stimulation results of Mädler and Coenen et al. (Mädler and Coenen, 2012), adapted depending on the respective pulse width (Dembek *et al.*, 2017). Finally, right-sided VTAs were nonlinearly flipped to the left hemisphere using Lead-DBS for further analysis (Al-Fatly *et al.*, 2019).

Functional connectivity estimation

To detect brain areas involved in SID we compared the functional connectivity of VTAs causing SID with those not causing SID, following a slightly modified approach as previously introduced by Al-Fatly et al. to investigate stimulation-induced side effects in essential tremor patients (Al-Fatly *et al.*, 2019). The functional connectivity of each VTA was estimated using the pipeline implemented in Lead-DBS. Here, we employed a functional connectome defined on resting state functional MRI scans of 1000 healthy subjects (https://data-verse.harvard.edu/datavers/GSP, (Yeo *et al.*, 2011)), which has previously been used to successfully predict tremor outcomes after thalamic DBS in essential tremor patients (Al-Fatly *et al.*, 2019). Data were collected with a 3T Siemens MRI scanner and the resting state blood oxygen level-dependent was processed with signal regression and application of spatial smoothing kernel of 6mm at full-width at half-maximum (Yeo *et al.*, 2011). Then all resulting functional connectivity maps were Fisher *z*-transformed before further analysis (Horn *et al.*, 2017). Statistical parametric mapping (SPM 12, Wellcome Department of Imaging Neuroscience, University College, London) was employed for second level analysis. Following an approach recently used by Reich et al., voxel-wise two-sample *t*-tests between connectivity strengths seeding from VTAs associated with SID and VTAs not associated with SID were calculated. SPM maps were obtained at a significance threshold of $p<0.05$ after family-wise error correction and a cluster extent of $k\geq100$ voxels (Reich *et al.*, 2016). The resulting connectivity difference image was created by voxel-wise subtractions of the mean connectivity

of VTAs not causing SID from the mean connectivity of VTAs causing SID, masked by the obtained clusters.

Determination of discriminative fibers

Determination of discriminative fibers for stimulation-induced worsening of intelligibility followed an approach introduced by Baldermann et al. (Baldermann *et al.*, 2019) based on a structural connectome (Horn *et al.*, 2014; Horn, 2015). This structural connectome has previously been used to successfully predict tremor outcomes after thalamic DBS in essential tremor patients (Al-Fatly *et al.*, 2019) and is based on diffusion data collected in 20 subjects using a single-shot spin-echo planar imaging sequence (repetition time = 10.000ms, echo time = 94ms, 2x2x2mm^3, 69 slices). Global fiber-tracking was performed using Gibb's tracking method (Reisert *et al.*, 2011), and the resulting fibers were warped into standard space (Horn and Blankenburg, 2016). In the present study, each of these fibers' discriminative value was tested by associating the fiber's connectivity to VTAs across patients with the respective change in intelligibility. Specifically, a linear mixed effect model was set up for each fiber connected to at least 20 VTAs, to test for significant differences between changes in speech intelligibility of connected and unconnected VTAs. The grouping variable (unconnected/connected) was included as a fixed-effect and the respective hemisphere was included as a random-effect, to reflect that two hemispheres were tested per patient. Change scores were calculated as percentage change from "OFF stimulation" state ((intelligibility$_{endpoint)}$– intelligibility$_{"OFFstimulation"}$)/intelligibility$_{"OFFstimulation"}$) and divided by the respective amplitude as proposed by Dembek et al., as changes in intelligibility in "ON stimulation state" were highly correlated with stimulation amplitude (rho = -0.66, p = 0.01 (Dembek *et al.*, 2017)). When connected VTAs led to worsening of speech intelligibility in comparison to unconnected VTAs with a p-value below 0.05, a fiber was determined as discriminative. Importantly, "ON stimulation" state VTAs were not included in the determination of discriminative fibers.

Validation of discriminative fibers

Discriminative fibers were validated in a leave-one-out design (Horn *et al.*, 2017; Al-Fatly *et al.*, 2019; Baldermann *et al.*, 2019). Briefly, discriminative fibers were recalculated for each patient based on the clinical assessments of all other patients ("leave-one-out" design). Then the respective number of discriminative fibers stimulated in the left-out patient's "ON stimulation" state was summed up to conduct a linear regression analysis. This was done to investigate the influence of the amount of discriminative fibers stimulated on the percentage change of intelligibility in the "ON stimulation" state. An additional linear regression analysis was conducted to investigate the influence of the amount of discriminative "speech"-fibers stimulated on postoperative tremor control, defined as the change in TRS hemiscores in "ON stimulation" compared to "OFF stimulation".

Technical realization

All computational work was carried out with MATLAB 2016b (TheMathWorksInc., Natick, Massachusetts, United States) on a DELL Precision T7910 Workstation with two Intel Xeon E5-2670 CPUs and 64 GB RAM (Dell Inc, Round Rock, Texas, United States). All atlas structures shown are taken from the DISTAL-atlas as implemented in LEAD-DBS (Ewert *et al.*, 2018).

Data availability

The data included in this study is available on reasonable request to the corresponding author. The data are not publicly available due to their containing information that could compromise the privacy of the participants.

Results

Patient characteristics

Fourteen patients diagnosed with essential tremor (four female) aged 65.4 (±13) years were prospectively recruited, resulting in 28 leads and 112 contacts investigated. Lead types and clinical stimulation settings are described in Supplementary Table 1. All patients were right-handed and bilaterally implanted either targeting the VIM (N = 2) or the VIM/PSA (Barbe *et al.*, 2018) (N = 12) with a mean time of 29.2 (±24) months since implantation.

Comparison of "OFF stimulation" and "ON stimulation" state

The mean rating of intelligibility did not differ significantly between "OFF stimulation" and "ON stimulation" state on the group level (mean OFF: 70.9 ±14.3, mean ON: 67.5 ±17.1, $p = 0.763$, Fig.1 A1). However, on the individual level, a formal worsening of intelligibility rating was observed in half of the patients. Regarding impairment of the speech motor system, syllable durations increased significantly during "ON stimulation" (mean OFF: 243ms ±58, mean ON: 275ms ±72, $p = 0.011$, Fig.1 B1). Regarding tremor control, TRS total scores improved significantly with clinical stimulation settings (mean OFF: 35.2 ±18.4, mean ON: 13.0 ±10.4, $p<0.001$, Fig.1 C1), reflecting a tremor suppression of over 60%.

Monopolar review outcomes

Figure 2 illustrates the anatomical position of investigated contacts and the stimulated region covering the VIM and the PSA. A total of 111 stimulation settings were included for further analysis (see Fig. 3). When comparing the "OFF stimulation" state to stimulation settings not causing SID and stimulation settings causing SID, Kruskal-Wallis test revealed differences in intelligibility ratings ($\chi^2(2) = 14.1$, $p<0.001$, Fig.1 A2). Post-hoc Wilcoxon rank-sum tests showed significant differences in "OFF" versus "SID" (mean "SID": 58.2 ±15.6, $p = 0.007$) and "no SID" versus "SID" (mean "no SID": 68.5 ±14.7, $p<0.001$). Additionally, for syllable durations Kruskal-Wallis test ($\chi^2(2) = 15.6$, $p<0.001$) and post-hoc Wilcoxon rank-sum tests

also revealed significant differences for “OFF” versus “SID” (mean “SID”: 293ms ±72, p = 0.011) and “no SID” versus “SID” (mean “no SID”: 247ms ±51, p<0.001). When assessing the ability to speak, significantly using the VAS, data suggested a significant worsening from “no SID” to “SID” (mean “no SID”: 2.0 ±2.0, mean “SID”: 3.9 ±2.0, p<0.001). When assessing postural tremor control, significantly using the VAS, data suggested significant improvement from “OFF” to “no SID” and “OFF” to “SID” (mean “OFF”: 5.9 ±1.6, mean “no SID”: 1.0 ±1.3, p<0.001; mean “SID”: 1.0 ±1.1, p<0.001). Intelligibility ratings significantly correlated to the patients’ VAS rating of their ability to speak (rho = -0.45, p<0.001), and syllable durations (rho = -0.66, p<0.001). As shown in Figure 3, onset of SID was associated with both, muscle contractions and/or ataxia, but also occurred without any additional symptoms.

Functional connectivity of VTAs causing stimulation-induced dysarthria

A total of 51 functional connectivity maps associated with SID and 60 functional connectivity maps not causing SID were included. The respective stimulation amplitudes did not differ significantly between the two groups (mean “no SID”: 5.6mA ±2.4, mean “SID”: 5.9mA ±1.8, p = 0.162). When comparing the functional connectivity of VTAs causing SID and VTAs not causing SID regarding the cerebral cortex, the connectivity difference image showed a stronger connectivity of VTAs causing SID to the precentral gyrus with a positive medio-lateral gradient, parts of the inferior and medial frontal gyrus, the supramarginal gyrus, and the superior temporal gyrus. For the cerebellar cortex, stronger connectivity of VTAs associated with SID was observed for the superior and the inferior cerebellar lobules, as well as the vermis (see Fig. 5).

Discriminative fibers for worsening of intelligibility

Fibers determined as discriminative for stimulation-induced worsening of intelligibility were mainly connected to the ipsilateral precentral gyrus as well as to both cerebellar hemispheres and the ipsilateral brainstem (see Fig. 5). In the target area, they ran laterally to the thalamus

and postero-medially to the subthalamic nucleus, in close proximity, mainly antero-laterally, to fibers beneficial for tremor control as published by Al-Fatly et al. (Al-Fatly *et al.*, 2019). Some of them even overlapped (see Fig. 6). Validation of the discriminative fibers in a leave-one-out design revealed that the overlap of the VTAs with the discriminative fibers identified in the present study could explain 33.2% of the variance in individual intelligibility outcome with clinical stimulation settings as measured in the respective "ON stimulation" state ($R^2 = 0.332$, $p = 0.031$, Fig. 5). Overlap of the VTAs with these discriminative "speech"-fibers was not associated with postoperative tremor control ($R^2 = 0.007$, $p = 0.662$).

Discussion

This study demonstrates that stimulation-induced speech impairment in thalamic DBS for essential tremor patients is associated with both, motor cortex and cerebellar cortex modulation and that DBS modulates the functional connectome of speech production. Furthermore, we were able to identify discriminative fibers predicting worsening of intelligibility in our cohort.

Modulation of the functional connectome of speech production by DBS

Following Fuertinger et al. (Fuertinger *et al.*, 2015) and Guenther et al. (Guenther and Vladusich, 2012) the functional connectome of real-life speech production in right-handed healthy subjects is constituted by a core hub network, centered on the left laryngeal and orofacial regions of the primary motor cortex and its main input regions in the surrounding premotor, somatosensory and parietal cortices. This core sensorimotor hub network is then widely connected to other brain regions such as the auditory cortex as an auditory feedback control subsystem, the parietal cortex for phonological and semantic processing, or the cerebellum for modulation of vocal motor timing and sequence processing (Ackermann *et al.*, 2007; Guenther and Vladusich, 2012; Price, 2012; Fuertinger *et al.*, 2015). In contrast to this real-life speech production network, the network involved in meaningless syllable production does not seem to include prefrontal cortex areas, pointing towards its specialized role in the

formation of cognitive aspects of speech control, such as verbal fluency (Schlosser *et al.*, 1998; Birn *et al.*, 2010; Fuertinger *et al.*, 2015).

The present study demonstrates that VTAs associated with SID have a higher connectivity to cortical areas forming part of the functional real-life speech production network than VTAs not associated with SID. As expected and hypothesized in previous studies (Astrom *et al.*, 2010; Mücke *et al.*, 2014; Becker *et al.*, 2017; Fenoy *et al.*, 2017; Mahlknecht *et al.*, 2017; Mücke *et al.*, 2018; Prent *et al.*, 2019), VTAs associated with SID were stronger connected to the primary motor cortex and the cerebellar cortex. The association between SID and these cortical areas is underlined by the fact that the onset of SID was in most of the cases associated with clinical symptoms of motor cortex modulation, i.e., muscle contractions, or cerebellar cortex involvement, i.e., ataxia (see Fig. 3). Notably, the distribution of voxels associated with SID followed the somatotopy of the precentral gyrus as well as the cerebellar cortex with higher connectivity values in cortical regions related to head and tongue control (Penfield and Boldrey, 1937; Buckner *et al.*, 2011) (see Fig. 4). Furthermore, cerebellar cortex modulation was especially observed in the superior paravermal region. Damage to this region has previously been reported to result in a slurred and poorly coordinated speech (Ackermann *et al.*, 1992), as also observed in essential tremor patients with deep brain stimulation (Mücke *et al.*, 2018; Hermes *et al.*, 2019). While an involvement of the precentral gyrus and the cerebellar cortex is in close relation to stimulation-induced deterioration of the speech motor system (Astrom *et al.*, 2010; Fenoy *et al.*, 2017; Mahlknecht *et al.*, 2017), consequences of a modulation of prefrontal, parietal, and temporal cortex remain more speculative. However, there might be a relation to auditory and somatosensory feedback mechanisms, located in the posterior end of the planum temporale and the supramarginal gyrus (Tourville *et al.*, 2008; Golfinopoulos *et al.*, 2011; Guenther and Vladusich, 2012), and to executive control, as assessed by verbal fluency, which has been reported to deteriorate under DBS in essential tremor patients (Ehlen *et al.*, 2014; Pedrosa *et al.*, 2014).

In contrast to the connectivity profile of VTAs associated with SID as identified by Al-Fatly et al. the connectivity profile of VTAs associated with SID as revealed in the present study is quite similar to the connectivity profile for optimal tremor control as described in their study (Al-Fatly *et al.*, 2019). These differences in the connectivity profiles for SID are most likely due to the fact, that Al-Fatly et al. only investigated clinical stimulation settings, resulting in only few dysarthric stimulation settings to be included in their analysis. However, the similarity of tremor- suppressing and SID inducing connectivity patterns underlines once more the proximity of these two effects and the need for a strategy to avoid SID while maintaining effective tremor control.

Discriminative fibers to predict worsening of intelligibility

Discriminative fibers for stimulation-induced worsening of intelligibility were identified to run laterally to the motor thalamus and postero-medially to the subthalamic nucleus. These fibers were either nearby, mainly antero-laterally, or even overlapping with fibers beneficial for tremor control as published by Al-Fatly et al. (Al-Fatly *et al.*, 2019). The overlap of the clinical stimulation settings with these fibers was predictive of 33.2% of the variance of stimulation-induced changes of intelligibility, as revealed by a leave-one-out design (see Fig. 5 and 6).

Intelligibility was chosen as a parameter representing the degree of SID in essential tremor patients since it indicates a deterioration of the speech motor system and represents the patient-rated “ability to speak”, and is therefore of high clinical relevance in daily living (Becker *et al.*, 2017). In contrast to previous studies, no worsening of intelligibility rating was observed with bilateral DBS on the group-level when comparing “On stimulation” and “Off stimulation” (Becker *et al.*, 2017; Becker *et al.*, 2020). This finding might be due to the fact that some patients in the present cohort had a voice tremor during “OFF stimulation” which can improve with DBS (Sandstrom *et al.*, 2019), and thereby might have led to an improvement of intelligibility beyond its worsening due to an affection of the glottal speech motor system (see

Fig. 1). In contrast, on the individual level, 50% of the patients experienced a worsening of intelligibility with clinical stimulation settings and there was a significant increase in syllable duration under DBS, indicating a systematic affection of the speech motor system in terms of oral control in our cohort.Of note, the identified fibers seem to be specific for changes in intelligibility as they were not predictive for tremor control.

In line with the functional connectivity profile of VTAs associated with SID, the discriminative fibers mainly connected the motor cortex to the brainstem and both cerebellar hemispheres. The course of these fibers also fits the finding of previous studies, reporting that a more lateral contact position (Becker *et al.*, 2017) and contacts located outside the motor thalamus are associated with SID in essential tremor patients (Matsumoto *et al.*, 2016). In contrast to these studies Fytagoridis et al. (Fytagoridis *et al.*, 2013) and Dembek et al. (Dembek *et al.*, 2017) detected no distinct patterns for contact positions or spread of stimulation in the thalamic area related to SID.

Interestingly, the course of the discriminative fibers is in line with a study by Aström et al.. The authors reported that a posteromedial contact position in relation to the subthalamic nucleus is associated with impairment of speech intelligibility in patients with Parkinson's disease treated with DBS of the subthalamic nucleus (Astrom *et al.*, 2010). Previous studies investigating changes in intelligibility after DBS of the subthalamic nucleus in Parkinson's disease provided evidence that both, modulation of motor fibers running in the internal capsule (Krack *et al.*, 2002; Mahlknecht *et al.*, 2017) and a modulation of cerebello-thalamic pathways, i.e., the dentatorubrothalamic tract (Fenoy *et al.*, 2017), can induce stimulation-induced speech worsening. Taking together the results of the present study and of previous studies providing evidence for a combination of spastic and atactic changes in the speech motor system (Mücke *et al.*, 2014; Mücke *et al.*, 2018), this pathophysiological correlate seems to hold true for SID in patients with ET. In contrast to DBS in Parkinson's disease the cerebello-thalamic-

subcircuits are not only relevant in the pathophysiology of stimulation-induced side effects, such as ataxia or speech changes, e.g. caused by a modulation of the cerebello-rubrospinal system and the fastigio-bulbar tract (Groppa *et al.*, 2014; Reich *et al.*, 2016), but are also crucial for the tremor-suppressing effect of DBS, especially related to the dentatorubrothalamic tract (Coenen *et al.*, 2014; Groppa *et al.*, 2014; Fenoy *et al.*, 2017). This anatomical proximity of tremor-suppressing effects and induction of dysarthria once more points toward the need for strategies to avoid SID to improve postoperative quality of life in essential tremor patients.

Methodological considerations and limitations

While previous studies focused on phonematic and articulographic features of SID (Kronenbuerger *et al.*, 2009; Mücke *et al.*, 2014; Becker *et al.*, 2017; Mücke *et al.*, 2018; Becker *et al.*, 2020) this study expands these findings by (1) revealing the networks underlying stimulation-induced dysarthria and (2) providing an atlas structure predictive of stimulation-induced changes in intelligibility. Furthermore, this study highlights the functional and structural proximity of tremor control and SID, which is often experienced in clinical practice and may lead to suboptimal postoperative tremor control. Although the cohort-size of fourteen patients might seem small, a total of 111 stimulation settings could be included in the analysis. To estimate the VTAs based on these stimulation settings, a well-established approach was used, that has previously been employed to identify optimal target regions and connectivity profiles in Parkinson's disease and essential tremor (Dembek *et al.*, 2017; Horn *et al.*, 2017; Al-Fatly *et al.*, 2019; Dembek *et al.*, 2019b; Petry-Schmelzer *et al.*, 2019). However, the theoretical concept of VTA modelling constitutes a simplification that neglects factors like fiber orientation (Anderson *et al.*, 2019). Regarding the concept of predicting effects of deep brain stimulation in relation to the anatomical target area there have been several approaches in the past, such as investigating lead positions (Delcour *et al.*, 2011; Camalier *et al.*, 2014; Barbe *et al.*, 2018; Dafsari *et al.*, 2018), the creation of probabilistic sweet spots (Eisenstein *et al.*, 2014; Dembek *et al.*, 2017; Dembek *et al.*, 2019b; Reich *et al.*, 2019), and the estimation of beneficial

connectivity profiles (Horn *et al.*, 2017; Al-Fatly *et al.*, 2019). In this study, we focused on providing an atlas structure that is easy to implement in planning and programming software and therefore decided to base our predictive model on an approach introduced by Baldermann et al. (Baldermann *et al.*, 2019).

Some methodological limitations should be considered when interpreting the results of this study. First, VTAs were pooled on the left hemisphere for the analysis. This approach seems appropriate as all patients were right-handed and previous studies did not show any difference between right and left hemispheric DBS regarding SID in bilaterally implanted essential tremor patients (Becker *et al.*, 2017). However, there are studies reporting SID to be associated with left-hemispheric stimulation of the subthalamic nucleus in Parkinson's disease (Tripoliti *et al.*, 2011; Tripoliti *et al.*, 2014). Second, an atlas-based approach neglects a certain degree of inter-individual heterogeneity, but the state-of-the-art multispectral co-registration approach used in this study has proved to be accurate (Ewert *et al.*, 2018; Ewert *et al.*, 2019). Third, this study employed normative connectome data to estimate seed-based connectivity in individual patients. This approach has already been implemented in many studies investigating the effects of DBS when patient-specific imaging data allowing fiber tracking was lacking, e.g., in Parkinson's disease and obsessive-compulsive disorder (Horn *et al.*, 2017; Baldermann *et al.*, 2019), but also essential tremor (Groppa *et al.*, 2014; Al-Fatly *et al.*, 2019). While these connectomes do not represent patient-specific connectivity, they are superior in quality to most images acquired during clinical routine by using specialized magnetic resonance hardware and best-performing tractography processing algorithms (Fillard *et al.*, 2011; Yeo *et al.*, 2011). Most importantly, using this specific normative connectome data allowed us to compare our results regarding SID to the results by Al-Fatly et al. regarding tremor suppression (Al-Fatly *et al.*, 2019) without being biased by different imaging acquisition protocols. Lastly, interindividual anatomical variability and center-specific targeting strategies might lead to different target points. This raises the question of the generalizability of our results to other

cohorts. Therefore, future studies, including different centers and target points, are warranted to create more generally applicable predictive models.

Conclusion

The present study demonstrates that both the motor cortex and the cerebellum are involved in the modulation of the functional connectome of speech motor production by deep brain stimulation in essential tremor patients. Furthermore, we were able to derive a fiber-based atlas structure, which could help to avoid stimulation-induced dysarthria in essential tremor patients and could easily be implemented in surgical planning as well as in postoperative programming.

Acknowledgments

The authors thank Bassam Al-Fatly and coworkers for providing the fibers associated with tremor control as published in Al-Fatly et al. 2019. In remembrance of Johannes Becker, whose enthusiasm, steadiness and criticism enriched this scientific field.

Funding

None.

Competing interests

The authors report no competing interests.

References

Ackermann H, Hertrich I, Hehr T. Oral diadochokinesis in neurological dysarthrias. Folia Phoniatr Logop 1995; 47(1): 15-23.

Ackermann H, Mathiak K, Riecker A. The contribution of the cerebellum to speech production and speech perception: clinical and functional imaging data. Cerebellum 2007; 6(3): 202-13.

Ackermann H, Vogel M, Petersen D, Poremba M. Speech deficits in ischaemic cerebellar lesions. J Neurol 1992; 239(4): 223-7.

Al-Fatly B, Ewert S, Kübler D, Kroneberg D, Horn A, Kühn AA. Connectivity profile of thalamic deep brain stimulation to effectively treat essential tremor. Brain 2019.

Anderson DN, Duffley G, Vorwerk J, Dorval AD, Butson CR. Anodic stimulation misunderstood: preferential activation of fiber orientations with anodic waveforms in deep brain stimulation. J Neural Eng 2019; 16(1): 016026.

Astrom M, Diczfalusy E, Martens H, Wardell K. Relationship between neural activation and electric field distribution during deep brain stimulation. IEEE Trans Biomed Eng 2015; 62(2): 664-72.

Astrom M, Tripoliti E, Hariz MI, Zrinzo LU, Martinez-Torres I, Limousin P, *et al.* Patient-specific model-based investigation of speech intelligibility and movement during deep brain stimulation. Stereotact Funct Neurosurg 2010; 88(4): 224-33.

Baldermann JC, Melzer C, Zapf A, Kohl S, Timmermann L, Tittgemeyer M, *et al.* Connectivity Profile Predictive of Effective Deep Brain Stimulation in Obsessive-Compulsive Disorder. Biol Psychiatry 2019; 85(9): 735-43.

Barbe MT, Dembek TA, Becker J, Raethjen J, Hartinger M, Meister IG, *et al.* Individualized current-shaping reduces DBS-induced dysarthria in patients with essential tremor. Neurology 2014; 82(7): 614-9.

Barbe MT, Reker P, Hamacher S, Franklin J, Kraus D, Dembek TA, *et al.* DBS of the PSA and the VIM in essential tremor: A randomized, double-blind, crossover trial. Neurology 2018; 91(6): e543-e50.

Becker J, Barbe MT, Hartinger M, Dembek TA, Pochmann J, Wirths J, *et al.* The Effect of Uni- and Bilateral Thalamic Deep Brain Stimulation on Speech in Patients With Essential Tremor: Acoustics and Intelligibility. Neuromodulation 2017; 20(3): 223-32.

Becker J, Thies T, Petry-Schmelzer JN, Dembek TA, Reker P, Mücke D, *et al.* The effects of thalamic and posterior subthalamic deep brain stimulation on speech in patients with essential tremor – A prospective, randomized, doubleblind crossover study. Brain and Language 2020; 202: 104724.

Birn RM, Kenworthy L, Case L, Caravella R, Jones TB, Bandettini PA, *et al.* Neural systems supporting lexical search guided by letter and semantic category cues: a self-paced overt response fMRI study of verbal fluency. Neuroimage 2010; 49(1): 1099-107.

Buckner RL, Krienen FM, Castellanos A, Diaz JC, Yeo BT. The organization of the human cerebellum estimated by intrinsic functional connectivity. J Neurophysiol 2011; 106(5): 2322-45.

Camalier CR, Konrad PE, Gill CE, Kao C, Remple MR, Nasr HM, *et al.* Methods for Surgical Targeting of the STN in Early-Stage Parkinson's Disease. Front Neurol 2014; 5: 25.

Coenen VA, Allert N, Paus S, Kronenburger M, Urbach H, Madler B. Modulation of the cerebello-thalamo-cortical network in thalamic deep brain stimulation for tremor: a diffusion tensor imaging study. Neurosurgery 2014; 75(6): 657-69; discussion 69-70.

Dafsari HS, Petry-Schmelzer JN, Ray-Chaudhuri K, Ashkan K, Weis L, Dembek TA, *et al.* Non-motor outcomes of subthalamic stimulation in Parkinson's disease depend on location of active contacts. Brain Stimul 2018; 11(4): 904-12.

Delcour M, Russier M, Xin DL, Massicotte VS, Barbe MF, Coq JO. Mild musculoskeletal and locomotor alterations in adult rats with white matter injury following prenatal ischemia. Int J Dev Neurosci 2011; 29(6): 593-607.

Dembek TA, Barbe MT, Astrom M, Hoevels M, Visser-Vandewalle V, Fink GR, *et al.* Probabilistic mapping of deep brain stimulation effects in essential tremor. Neuroimage Clin 2017; 13: 164-73.

Dembek TA, Hoevels M, Hellerbach A, Horn A, Petry-Schmelzer JN, Borggrefe J, *et al.* Directional DBS leads show large deviations from their intended implantation orientation. Parkinsonism Relat Disord 2019a; 67: 117-21.

Dembek TA, Roediger J, Horn A, Reker P, Oehrn C, Dafsari HS, *et al.* Probabilistic sweet spots predict motor outcome for deep brain stimulation in Parkinson disease. Ann Neurol 2019b; 86(4): 527-38.

Deuschl G, Bain P, Brin M. Consensus statement of the Movement Disorder Society on Tremor. Ad Hoc Scientific Committee. Mov Disord 1998; 13 Suppl 3: 2-23.

Ehlen F, Schoenecker T, Kuhn AA, Klostermann F. Differential effects of deep brain stimulation on verbal fluency. Brain Lang 2014; 134: 23-33.

Eisenstein SA, Koller JM, Black KD, Campbell MC, Lugar HM, Ushe M, *et al.* Functional anatomy of subthalamic nucleus stimulation in Parkinson disease. Ann Neurol 2014; 76(2): 279-95.

Ewert S, Horn A, Finkel F, Li N, Kuhn AA, Herrington TM. Optimization and comparative evaluation of nonlinear deformation algorithms for atlas-based segmentation of DBS target nuclei. Neuroimage 2019; 184: 586-98.

Ewert S, Plettig P, Li N, Chakravarty MM, Collins DL, Herrington TM, *et al.* Toward defining deep brain stimulation targets in MNI space: A subcortical atlas based on multimodal MRI, histology and structural connectivity. Neuroimage 2018; 170: 271-82.

Fenoy AJ, McHenry MA, Schiess MC. Speech changes induced by deep brain stimulation of the subthalamic nucleus in Parkinson disease: involvement of the dentatorubrothalamic tract. J Neurosurg 2017; 126(6): 2017-27.

Fenoy AJ, Schiess MC. Deep Brain Stimulation of the Dentato-Rubro-Thalamic Tract: Outcomes of Direct Targeting for Tremor. Neuromodulation 2017; 20(5): 429-36.

Fillard P, Descoteaux M, Goh A, Gouttard S, Jeurissen B, Malcolm J, *et al.* Quantitative evaluation of 10 tractography algorithms on a realistic diffusion MR phantom. Neuroimage 2011; 56(1): 220-34.

Flora ED, Perera CL, Cameron AL, Maddern GJ. Deep brain stimulation for essential tremor: a systematic review. Mov Disord 2010; 25(11): 1550-9.

Fuertinger S, Horwitz B, Simonyan K. The Functional Connectome of Speech Control. PLoS Biol 2015; 13(7): e1002209.

Fytagoridis A, Astrom M, Wardell K, Blomstedt P. Stimulation-induced side effects in the posterior subthalamic area: distribution, characteristics and visualization. Clin Neurol Neurosurg 2013; 115(1): 65-71.

Golfinopoulos E, Tourville JA, Bohland JW, Ghosh SS, Nieto-Castanon A, Guenther FH. fMRI investigation of unexpected somatosensory feedback perturbation during speech. Neuroimage 2011; 55(3): 1324-38.

Groppa S, Herzog J, Falk D, Riedel C, Deuschl G, Volkmann J. Physiological and anatomical decomposition of subthalamic neurostimulation effects in essential tremor. Brain 2014; 137(Pt 1): 109-21.

Guenther FH, Vladusich T. A Neural Theory of Speech Acquisition and Production. Journal of neurolinguistics 2012; 25(5): 408-22.

Hermes A, Mücke D, Thies T, Barbe MT. Coordination patterns in Essential Tremor patients with Deep Brain Stimulation: Syllables with low and high complexity. Laboratory Phonology: Journal of the Association for Laboratory Phonology 2019; 10(1).

Horn A. A structural group-connectome in standard stereotactic (MNI) space. Data Brief 2015; 5: 292-6.

Horn A, Blankenburg F. Toward a standardized structural-functional group connectome in MNI space. Neuroimage 2016; 124(Pt A): 310-22.

Horn A, Li N, Dembek TA, Kappel A, Boulay C, Ewert S, *et al.* Lead-DBS v2: Towards a comprehensive pipeline for deep brain stimulation imaging. Neuroimage 2019; 184: 293-316.

Horn A, Ostwald D, Reisert M, Blankenburg F. The structural-functional connectome and the default mode network of the human brain. Neuroimage 2014; 102 Pt 1: 142-51.

Horn A, Reich M, Vorwerk J, Li N, Wenzel G, Fang Q, *et al.* Connectivity predicts deep brain stimulation outcome in Parkinson's disease. Ann Neurol 2017.

Husch A, M VP, Gemmar P, Goncalves J, Hertel F. PaCER - A fully automated method for electrode trajectory and contact reconstruction in deep brain stimulation. Neuroimage Clin 2018; 17: 80-9.

Johnson H, Harris G, Williams K. BRAINSFit: Mutual Information Registrations of Whole-Brain 3D Images, Using the Insight Toolkit. 2007.

Krack P, Dostrovsky J, Ilinsky I, Kultas-Ilinsky K, Lenz F, Lozano A, *et al.* Surgery of the motor thalamus: problems with the present nomenclatures. Mov Disord 2002; 17 Suppl 3: S2-8.

Kronenbuerger M, Konczak J, Ziegler W, Buderath P, Frank B, Coenen VA, *et al.* Balance and motor speech impairment in essential tremor. Cerebellum 2009; 8(3): 389-98.

Louis ED, Ferreira JJ. How common is the most common adult movement disorder? Update on the worldwide prevalence of essential tremor. Mov Disord 2010; 25(5): 534-41.

Mädler B, Coenen VA. Explaining clinical effects of deep brain stimulation through simplified target-specific modeling of the volume of activated tissue. AJNR Am J Neuroradiol 2012; 33(6): 1072-80.

Mahlknecht P, Akram H, Georgiev D, Tripoliti E, Candelario J, Zacharia A, *et al.* Pyramidal tract activation due to subthalamic deep brain stimulation in Parkinson's disease. Mov Disord 2017; 32(8): 1174-82.

Matsumoto JY, Fossett T, Kim M, Duffy JR, Strand E, McKeon A, *et al.* Precise stimulation location optimizes speech outcomes in essential tremor. Parkinsonism Relat Disord 2016; 32: 60-5.

Mücke D, Becker J, Barbe MT, Meister I, Liebhart L, Roettger TB, *et al.* The effect of deep brain stimulation on the speech motor system. J Speech Lang Hear Res 2014; 57(4): 1206-18.

Mücke D, Hermes A, Roettger TB, Becker J, Niemann H, Dembek TA, *et al.* The effects of Thalamic Deep Brain Stimulation on speech dynamics in patients with Essential Tremor: An articulographic study. PLoS One 2018; 13(1): e0191359.

Pahwa R, Lyons KE, Wilkinson SB, Simpson RK, Jr., Ondo WG, Tarsy D, *et al.* Long-term evaluation of deep brain stimulation of the thalamus. J Neurosurg 2006; 104(4): 506-12.

Pedrosa DJ, Auth M, Pauls KA, Runge M, Maarouf M, Fink GR, *et al.* Verbal fluency in essential tremor patients: the effects of deep brain stimulation. Brain Stimul 2014; 7(3): 359-64.

Penfield W, Boldrey E. Somatic motor and sensory representation in the cerebral cortex of man as studied by electrical stimulation. Brain 1937; 60(4): 389-443.

Petry-Schmelzer JN, Krause M, Dembek TA, Horn A, Evans J, Ashkan K, *et al.* Non-motor outcomes depend on location of neurostimulation in Parkinson's disease. Brain 2019; 142(11): 3592-604.

Prent N, Potters WV, Boon LI, Caan MWA, de Bie RMA, van den Munckhof P, *et al.* Distance to white matter tracts is associated with deep brain stimulation motor outcome in Parkinson's disease. J Neurosurg 2019: 1-10.

Price CJ. A review and synthesis of the first 20 years of PET and fMRI studies of heard speech, spoken language and reading. Neuroimage 2012; 62(2): 816-47.

Reich MM, Brumberg J, Pozzi NG, Marotta G, Roothans J, Astrom M, *et al.* Progressive gait ataxia following deep brain stimulation for essential tremor: adverse effect or lack of efficacy? Brain 2016.

Reich MM, Horn A, Lange F, Roothans J, Paschen S, Runge J, *et al.* Probabilistic mapping of the antidystonic effect of pallidal neurostimulation: a multicentre imaging study. Brain 2019; 142(5): 1386-98.

Reisert M, Mader I, Anastasopoulos C, Weigel M, Schnell S, Kiselev V. Global fiber reconstruction becomes practical. Neuroimage 2011; 54(2): 955-62.

Sandstrom L, Blomstedt P, Karlsson F. Voice Tremor Response to Deep Brain Stimulation in Relation to Electrode Location in the Posterior Subthalamic Area. World Neurosurg X 2019; 3: 100024.

Schlosser R, Hutchinson M, Joseffer S, Rusinek H, Saarimaki A, Stevenson J, *et al.* Functional magnetic resonance imaging of human brain activity in a verbal fluency task. J Neurol Neurosurg Psychiatry 1998; 64(4): 492-8.

Schuurman PR, Bosch DA, Bossuyt PM, Bonsel GJ, van Someren EJ, de Bie RM, *et al.* A comparison of continuous thalamic stimulation and thalamotomy for suppression of severe tremor. N Engl J Med 2000; 342(7): 461-8.

Tourville JA, Reilly KJ, Guenther FH. Neural mechanisms underlying auditory feedback control of speech. Neuroimage 2008; 39(3): 1429-43.

Tripoliti E, Limousin P, Foltynie T, Candelario J, Aviles-Olmos I, Hariz MI, *et al.* Predictive factors of speech intelligibility following subthalamic nucleus stimulation in consecutive patients with Parkinson's disease. Mov Disord 2014; 29(4): 532-8.

Tripoliti E, Zrinzo L, Martinez-Torres I, Frost E, Pinto S, Foltynie T, *et al.* Effects of subthalamic stimulation on speech of consecutive patients with Parkinson disease. Neurology 2011; 76(1): 80-6.

Yeo BT, Krienen FM, Sepulcre J, Sabuncu MR, Lashkari D, Hollinshead M, *et al.* The organization of the human cerebral cortex estimated by intrinsic functional connectivity. J Neurophysiol 2011; 106(3): 1125-65.

Figures

Figure 1 – Clinical assessments

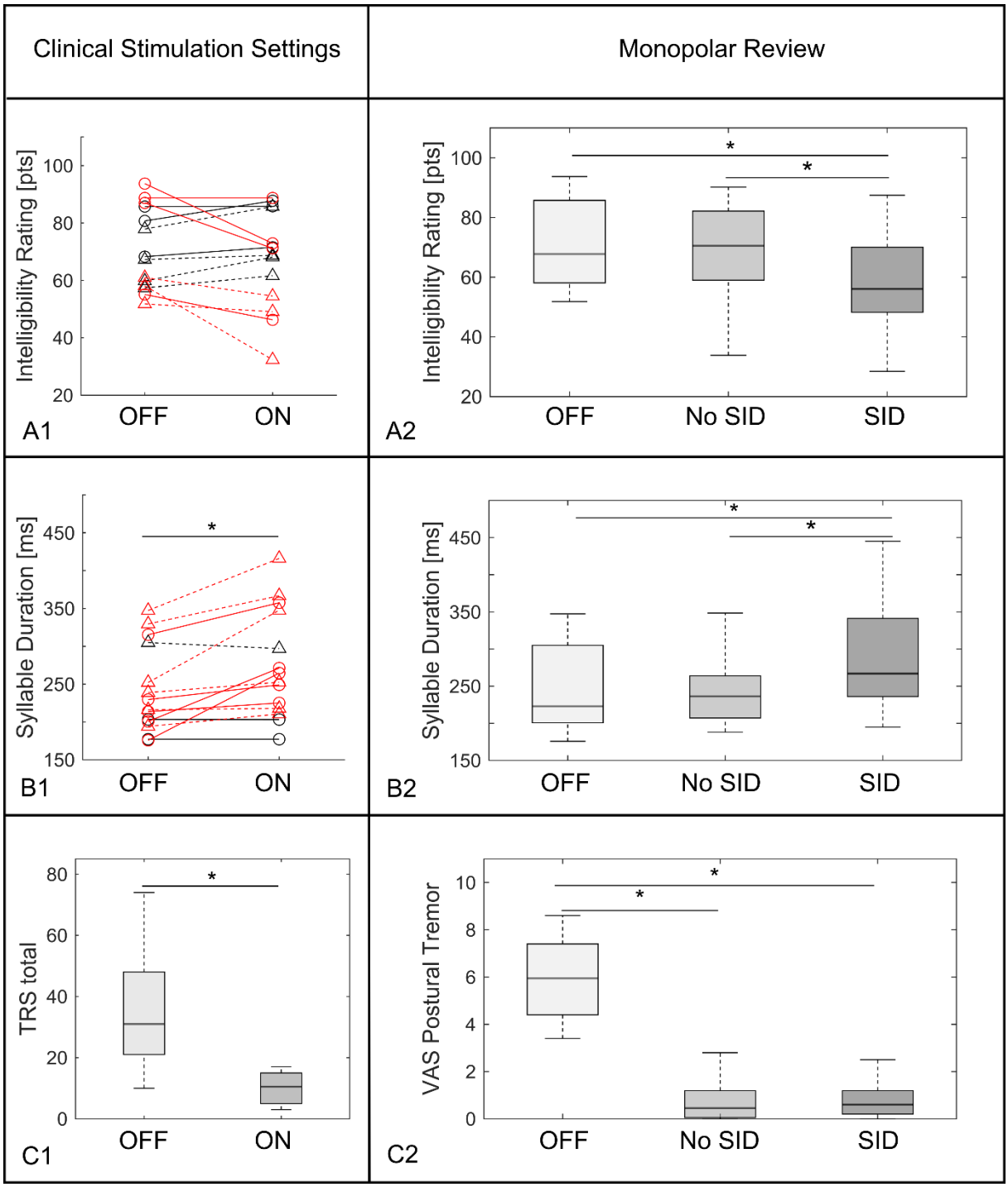

Fig. 1 - Clinical assessments. Comparison of "OFF stimulation" and "ON stimulation" states (column one) and comparison of "OFF stimulation" state, stimulation settings not causing stimulation-induced dysarthria (SID) and stimulation settings causing SID during monopolar review (column two) for intelligibility rating (A), syllable duration (B) and tremor ratings (C). Black stars indicate significant differences ($p<0.05$) between the settings. Triangles in column

one indicate the appearance of voice tremor in the “OFF stimulation” state and individual formal worsening is marked in red.

Abbreviations: SID = stimulation-induced dysarthria, **TRS** = tremor rating scale; **VAS** = visual analog scale

Figure 2 – Contact positions and investigated anatomical area

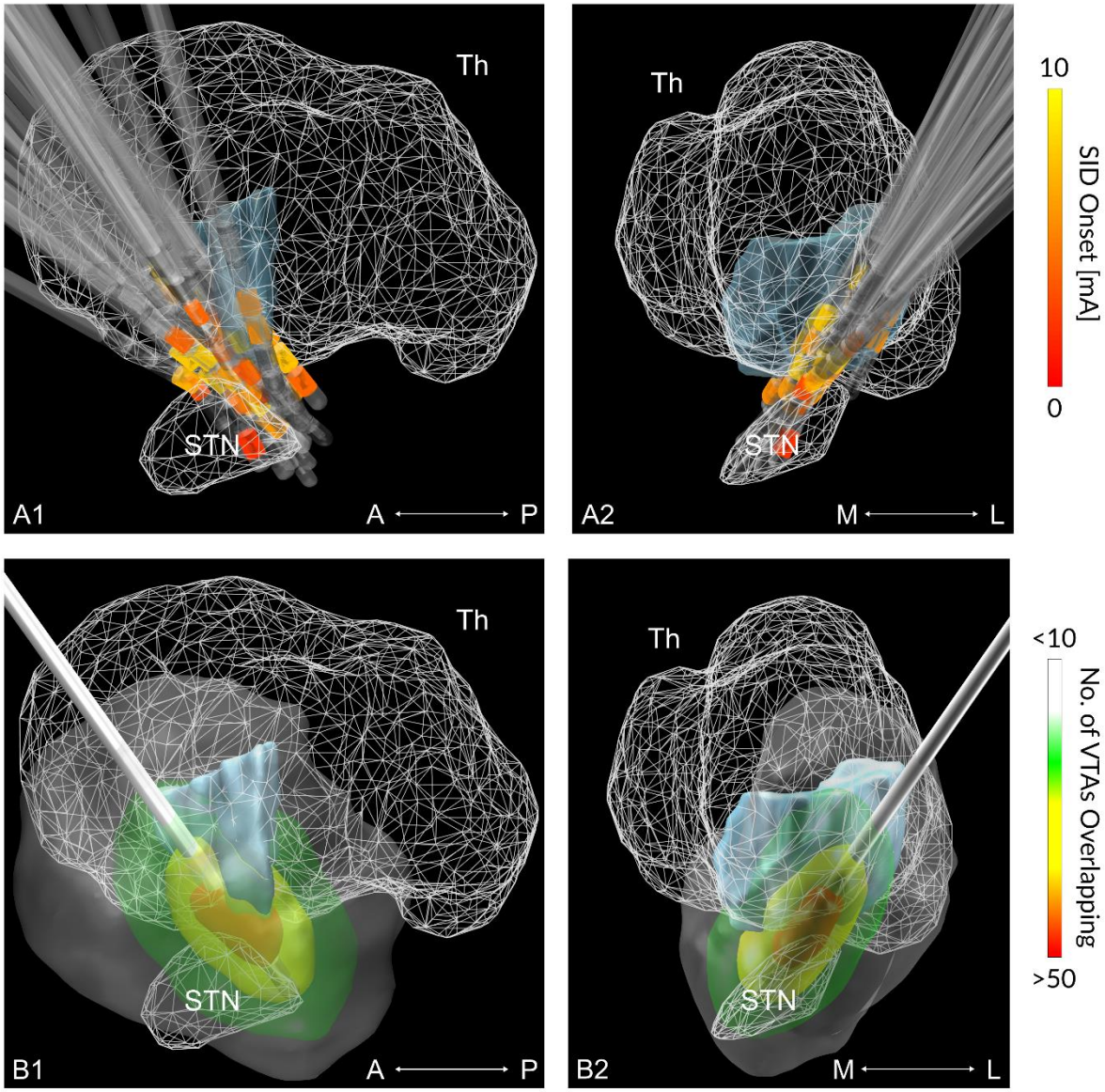

Fig. 2 – Contact positions and investigated anatomical area. (A) shows the positions of left-pooled contacts included in the analysis in standard space (ICBM 2009b NLIN, Asym) in lateral (A1) and anterior view (A2) together with the thalamus, the VIM (blue), and the STN. Contacts at which stimulation-induced dysarthria could be provoked are color-coded by the amplitude at the onset of dysarthria. (B) illustrates the investigated anatomical area together with the mean lead position in lateral (B1) and anterior view (B2), together with the thalamus, the VIM (blue), and the STN. Anatomical structures are taken from the DISTAL atlas, as included in LEAD-DBS (Ewert *et al.*, 2018; Horn *et al.*, 2019).

Abbreviations: **A** = anterior, **L** = lateral, **M** = medial, **P** = posterior, **STN** = nucleus subthalamicus, **Th** = thalamus, **VIM** = ventral intermediate nucleus, **VTA** = volume of tissue activated

Figure 3 – Clinical symptoms associated with stimulation-induced dysarthria

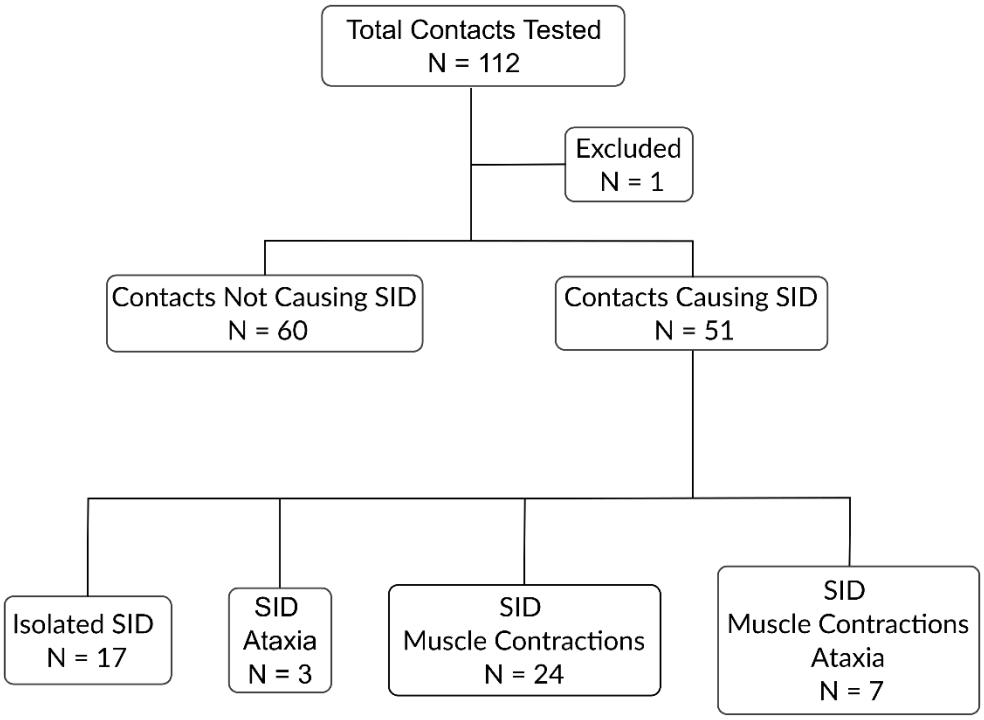

Fig. 3 – Clinical symptoms associated with stimulation-induced dysarthria. Clinical symptoms of motor cortex (muscle contractions) or cerebellar cortex (ataxia) involvement at the onset of stimulation-induced dysarthria (SID). One contact was excluded as the patient experienced side effects severely interfering with further testing.

Abbreviations: SID = stimulation-induced dysarthria

Figure 4 – Cortical areas associated with stimulation-induced dysarthria

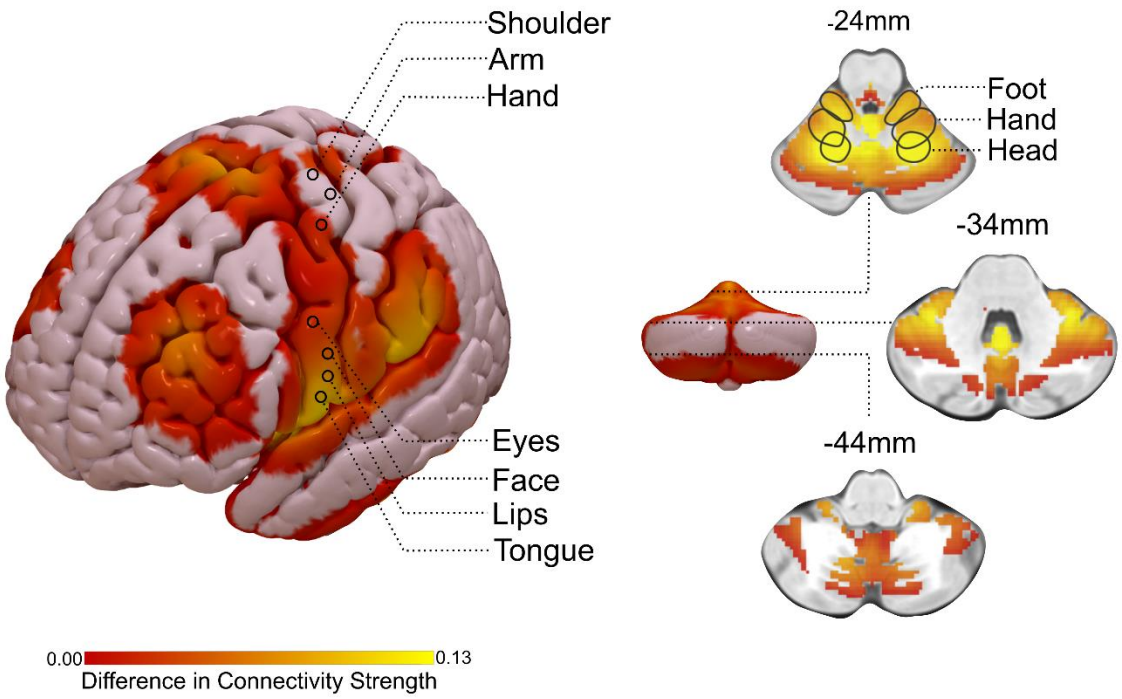

Fig. 4 – Cortical areas associated with stimulation-induced dysarthria. Cerebral and cerebellar cortex connectivity difference image of VTAs not causing dysarthria and VTAs causing dysarthria as identified in a high definition functional connectome (Yeo *et al.*, 2011) together with the respective topographic organization (Penfield and Boldrey, 1937; Buckner *et al.*, 2011). As indicated by the color bar, more yellow areas represent stronger connectivity to VTAs causing dysarthria. 2D slices are shown in axial view with indication of the respective z-values.

Abbreviations: VTA = volume of tissue activated

Figure 5 – Discriminative fibers for speech intelligibility

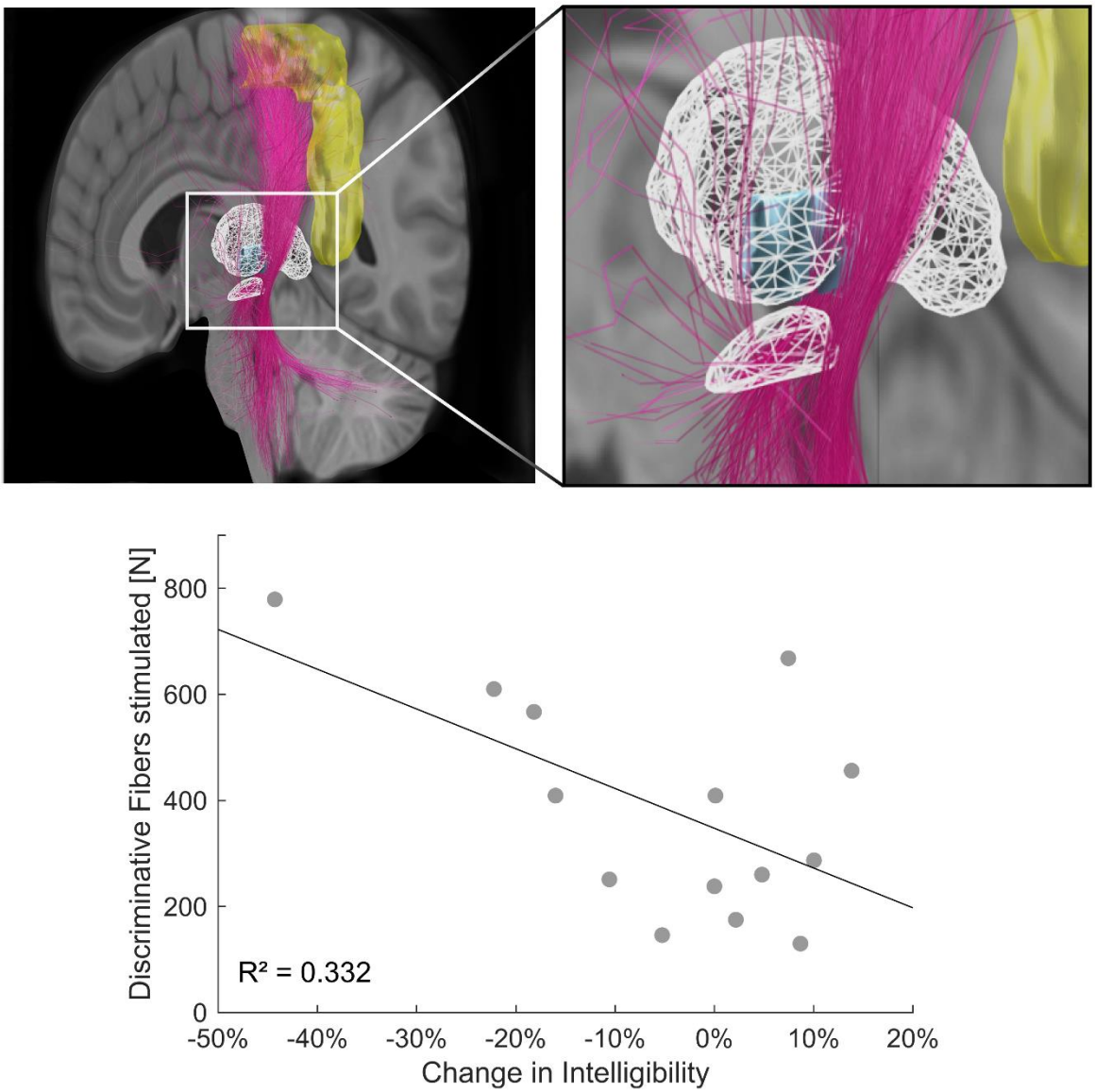

Fig. 5 Discriminative fibers for speech intelligibility. The course of discriminative fibers for stimulation-induced changes in intelligibility (pink) as identified in a high-definition structural connectome (Horn *et al.*, 2014; Horn, 2015). Fibers are shown in the antero-lateral view together with the thalamus, the VIM (blue), the precentral gyrus (yellow), and the STN. Discriminative fibers were validated in a leave-one-out design, explaining 33.2% of the variance in change of intelligibility during "ON stimulation" ($p = 0.031$).

Abbreviations: STN = nucleus subthalamicus, **VIM** = ventral intermediate nucleus

Figure 6 – Comparison of discriminative fibers for changes of intelligibility and tremor control

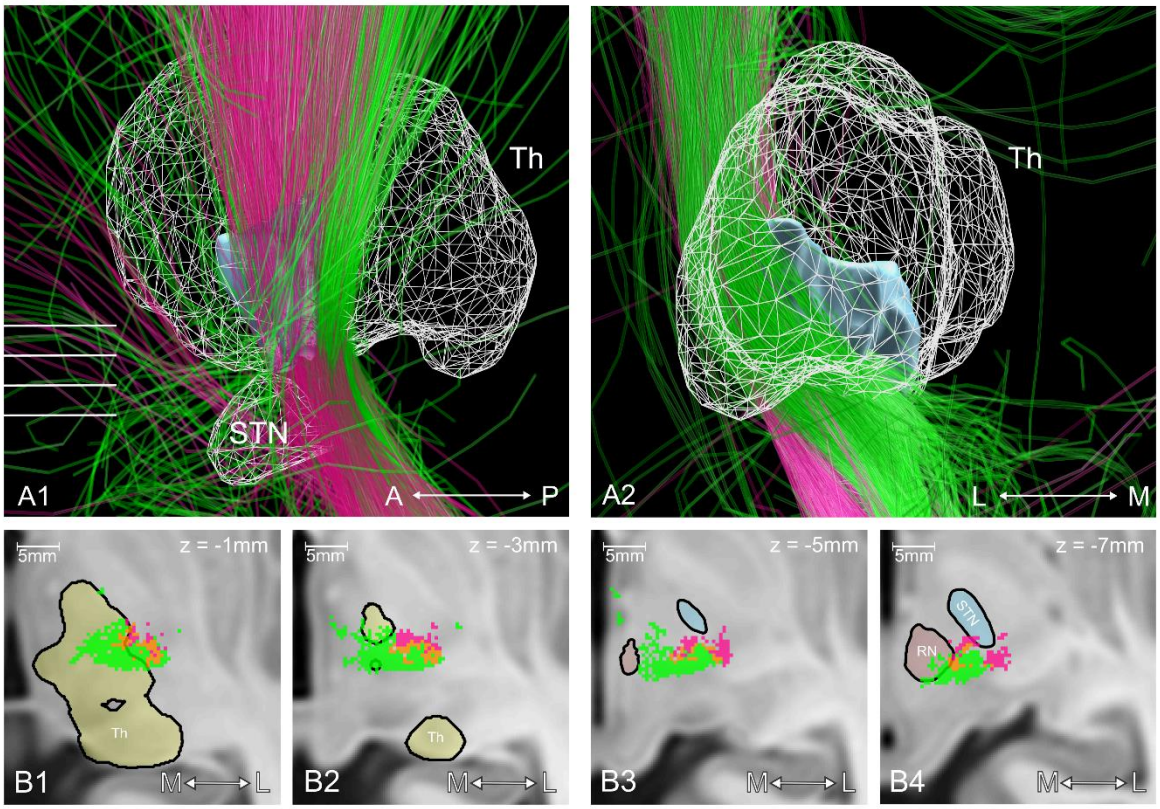

Fig. 6 - Comparison of discriminative fibers for changes of intelligibility and tremor control. The course of discriminative fibers for changes of intelligibility (pink) and postoperative tremor control (green) in lateral (A1) and posterior view (A2), together with the thalamus, the VIM (blue), and the STN. (B) illustrates the course of the respective fibers in axial view with overlapping areas marked in orange. Slice positions are indicated in A1. For increased clarity only voxels with at least six neighbored voxels containing the respective fiber tracts are shown.

Abbreviations: A = anterior, **L** = lateral, **M** = medial, **P** = posterior, **RN** = red nucleus, **STN =** nucleus subthalamicus, **Th** = thalamus, **VIM** = ventral intermediate nucleus

Supplementary Materials

Supplementary Table 1 – Clinical stimulation settings

Patient	Lead type	Clinical stimulation settings	
		Left hemisphere	Right hemisphere
1	Cartesia™, Boston Scientific	C+, 2- 21%, 3- 5%, 4- 29%, 5- 17%,6- 5%,7- 23%, 60µs, 149Hz, 2.3mA	C+, 10- 17%, 11- 26%, 12- 27%, 13- 10%, 14- 10%, 15- 10%, 60µs, 149Hz, 2.3mA
2	Cartesia™, Boston Scientific	5+34%, 6+ 33%, 7+ 33%, 1- 90%, 2- 5%, 4- 5%, 40µs, 204Hz, 5.0mA	13+ 34%, 14+ 33%, 15+ 33%, 9- 80%, 11- 10%, 12- 10%, 40µs, 204Hz, 4.7mA
3	Medtronic 3387, Medtronic	C+, 1- 100%, 60µs, 180Hz, 3.0mA	C+, 9- 100%, 60µs, 180Hz, 1.9mA
4	Cartesia™, Boston Scientific	C+, 2- 100%, 60µs, 130Hz, 3.6mA	C+, 10- 29%, 11- 43%, 12- 28%, 60µs, 130Hz, 1.9mA
5	Cartesia™, Boston Scientific	C+, 2- 34%, 3- 33%, 4- 33%, 60µs, 130Hz, 2.1mA	C+, 10- 34%, 11- 33%, 12- 33%, 60µs, 130Hz, 2.1mA
6	Vercise™, Boston Scientific	C+, 3- 100%, 60µs, 130Hz, 3.2mA	C+, 11- 100%, 60µsec, 174Hz, 2.3mA
7	Medtronic 3389, Medtronic	C+, 2- 100%, 60µs, 130Hz, 3.7mA	C+, 10- 100%, 60µs, 130Hz, 2.0mA
8	Vercise™, Boston Scientific	C+, 3- 100%, 60µs, 174 Hz, 1.3mA	C+, 11- 100%, 60µsec, 174Hz, 0.7mA
9	Vercise™, Boston Scientific	C+, 3- 100%, 60µs, 130Hz, 3.8mA	C+, 11-, 100%, 60µs, 130Hz, 2.9mA
10	Medtronic 3389, Medtronic	Vim 1: C+, 0-, 2.0V, 60µs, 125Hz Vim 2: C+, 1-, 2.5V, 60µs, 125Hz	Vim 1: C+, 8-, 2.0V, 60µs, 125Hz Vim 2: C+, 9-, 2.7V, 60µs, 125 Hz
11	Vercise™, Boston Scientific	5+ 100%, 2- 70%, 3- 30%, 60µs, 174Hz, 2.1mA	13+ 100%, 10- 70%, 11- 30%, 60µs, 174Hz, 2.1mA
12	Cartesia™, Boston Scientific	C+, 1- 100%, 50µs, 185Hz, 1.4mA	C+, 13- 35%, 14- 35%, 15- 30%, 60µs, 185Hz, 1,2mA
13	Cartesia™, Boston Scientific	C+, 2- 34%, 3- 33%, 4- 33%, 60µs, 185Hz, 1.2mA	C+, 10- 34%, 11- 33%, 12- 33%, 60µs, 185Hz, 1.6mA
14	Cartesia™, Boston Scientific	C+, 1- 100%, 60µs, 130 Hz, 1.2mA	C+, 9- 100%, 60µs, 130Hz, 1.2mA